Bioorganic Chemistry 166 (2025) 109128

Contents lists available at ScienceDirect

Bioorganic Chemistry

journal homepage: www.elsevier.com/locate/bioorg

Discovery of new neutrophil elastase inhibitors through Meloidae genome and transcriptome analyses

Marianna Nicoletta Rossi [a], Lavinia Attili [a], Cristian Fiorucci [a], William Fabiani [a], Sarah Andreucci [a], Paolo Franchini [b], Alessandra Riccieri [a,c], Lucrezia Spagoni [a,d], Marco Alberto Bologna [a,c], Guglielmo Duranti [e], Roberta Ceci [e], Emiliano Fratini [f], Kathleen Carleer [g], Jan Tytgat [g], Fabio Polticelli [a], Manuela Cervelli [a,*]

[a] Roma Tre University, Department of Sciences, Rome, Italy
[b] University of Tuscia Department of Biological and Ecological Sciences, Viterbo, Italy
[c] NBFC, National Biodiversity Future Center, Palermo, Italy
[d] Stazione Zoologica Anton Dohrn Calabria Marine Centre (CRIMAC), Department of Integrative Marine Ecology (EMI), Amendolara, Cosenza, Italy
[e] University of Rome Foro Italico, Department of Movement, Human and Health Sciences, Rome, Italy
[f] ENEA Casaccia Research Centre, Division of Biotechnologies, Italian National Agency for New Technologies, Energy and Sustainable Economic Development, Rome, Italy
[g] KU Leuven, Department of Pharmaceutical and Pharmacological Sciences, Leuven, Belgium

ARTICLE INFO

Dataset link: Meloidae KPI versus elastase (Original data)

Keywords:
Kunitz
Elastase
NETs
Protease inhibitors
Bioactive compounds

ABSTRACT

Neutrophil elastase (NE), a serine protease secreted by activated neutrophils, is a key regulator of inflammation and tissue damage. Among natural NE regulators, Kunitz-type serine protease inhibitors have attracted considerable attention for their therapeutic potential. In this study, integrated transcriptomic and genomic analyses of the blister beetles *Lydus trimaculatus* and *Mylabris variabilis*, led to the identification of four novel Kunitz-type inhibitors, Lyd_37798, Myl_35212i1, Myl_17096, and Myl_35212i2 with Ki values against NE of 32.36 nM, 76.45 nM, 154.5 nM, and 754.3 nM, respectively. While all peptides show a conserved Kunitz scaffold, they differ in their P1 residues, suggesting functional diversity. Notably, the most potent inhibitor, Lyd_37798, displays an uncommon aspartic acid at the P1 position, proposing new insights for the design of elastase-target drugs. Structural modelling demonstrated that these peptides bind NE with a reactive loop closely resembling that of the known elastase-specific inhibitor Elafin. Functionally, Lyd_37798 (P1 Asp) and Myl_17096 (P1 Lys) significantly suppressed the formation of neutrophil extracellular traps (NETs), reducing NET release by 89.2 % and 86.9 % respectively. Both peptides also revealed high specificity for NE, without affecting a broad spectrum of cellular ion channels, suggesting a favourable safety profile. Overall, this study highlights the unexploited potential of insect-derived Kunitz peptides as a valuable source of selective NE inhibitors and lays the foundation for their development as therapeutic drugs against NE-mediated inflammatory and degenerative diseases.

1. Introduction

1.1. Kunitz peptide inhibitors

Kunitz peptide inhibitors (KPI), named after the American physiologist and biochemist Maurice M. Kunitz who first identified them in the 1940s [1], represent a fascinating class of naturally occurring protease inhibitors found in various organisms across the biological spectrum. They are small proteins that inhibit serine proteases with a distinctive structure, typically comprising approximately 50–60 amino acids and stabilized by disulfide bonds, which confer a high degree of stability [2,3]. The Kunitz domain is found in a variety of organisms and serves crucial roles in regulating proteolytic activity, thereby influencing processes such as blood coagulation, inflammation, and tissue remodelling [4,5]. They bind to their target enzymes with high affinity, effectively blocking the active site and preventing substrate cleavage [4].

1.2. Elastase is a serine protease

Elastase is a serine protease enzyme that hydrolyses collagen,

* Corresponding author.
E-mail address: manuela.cervelli@uniroma3.it (M. Cervelli).

https://doi.org/10.1016/j.bioorg.2025.109128
Received 22 July 2025; Received in revised form 16 October 2025; Accepted 19 October 2025
Available online 22 October 2025

proteoglycan and elastin, key proteins of the extracellular matrix that provides elasticity to organs such as skin, lungs, and blood vessels. Elastase is produced by various cells, including neutrophils and pancreatic acinar cells, and plays an important role in tissue remodelling and host defence mechanisms [6]. In neutrophils, elastase is stored in granules and released upon their activation, contributing to the breakdown of extracellular matrix components during inflammation and infection [7–10]. Dysregulation of elastase activity, however, can lead to pathological conditions, such as chronic obstructive pulmonary disease (COPD) and emphysema, where excessive elastin degradation results in loss of tissue elasticity and function [11,12].

1.3. Neutrophil elastase and NETosis

Neutrophil elastase (NE) activity plays a crucial role in a distinctive form of cell death known as NETosis, which is specific to neutrophils. During this process, neutrophils release Neutrophil extracellular traps (NET) networks composed mainly of DNA, histones, and granule proteins, to trap and neutralize pathogens. While NET formation is essential for host defence, excessive NET release can contribute to tissue damage and excessive inflammation. These pathological effects have been observed in the context of COVID-19, where NETs are implicated in disease severity and complications [13–17]. An important role of elastase and neutrophils has also been described in cancer progression where NE activates dormant cancer cells, promotes tumour cell proliferation and distant metastasis, and changes the tumour microenvironment [6,18]. Due to the importance of NE in human physiopathology, inhibitors that specifically act on this protease have great pharmacological interests [19–22].

1.4. Kunitz peptide inhibitors from insects

In insects, KPIs perform a variety of critical roles. These include defence mechanisms against predators and pathogens, regulation of proteolytic cascades in processes like blood coagulation and immune responses, and modulation of developmental pathways [23–26]. The multifunctionality of KPIs in insects highlights their evolutionary significance and the potential for diverse applications. The developments in biotechnology and molecular biology have facilitated the exploration of KPIs from insects for medical purpose [26–30]. Inhibitors derived from insects have shown promise in the development of novel treatments for cancer, inflammation, and neurodegenerative disorders. In insects, serine protease inhibitors regulate the proteolytic cascades involved in haemolymph coagulation, thus contributing to the innate immune responses [23,31]. This coagulation process, similarly to the blood clotting mechanism in human, involves a series of serine proteases whose activities are tightly controlled to maintain physiological balance and prevent excessive clot formation. Insects from the beetle family Meloidae, commonly known as blister beetles (Coleoptera: Meloidae), employ a unique defence mechanism: when threatened, they exude yellowish, oily droplets of haemolymph from their leg joints. This secretion contains cantharidin, a potent terpenoid toxin that serves as a powerful deterrent against predators [32,33]. To avoid excessive haemolymph loss during this process, these beetles have developed a tight and reversible coagulation control system. The presence of KPIs in their system likely plays a crucial role in this regulation, guaranteeing effective defence while preserving physiological balance. The possible more physiological role of Meloidea derived KPI prompted us to investigate their activity. This is a strong differences from many other Kunitz inhibitors that are components of the venoms of poisonous or hematophagous animals including snakes, sea anemones, scorpions, ticks and others [4] or are expressed by plants as defence against pests and pathogens [34]. We reasoned that when an inhibitor evolves to regulate the organism's own physiology, it needs to act in a precise, fine-tuned way to control a specific process. This means that such an inhibitor will likely be specific and potent enough to affect its target but not so powerful that it causes harm to the organism itself.

Previous transcriptomic analyses of two blister beetle species, *Mylabris variabilis* and *Lydus trimaculatus*, revealed a set of genes encoding proteins with potential anticoagulant activity [35]. Among these, KPIs were identified, which may contribute to the autohaemorrhaging defence strategy. In this study, an integrated transcriptomic and genomic approach led to the identification of potential KPI from two meloidae insects species *Lydus trimaculatus* and *Myrabilis variabilis*. Through a combination of *in silico* and *in vitro* assays we characterized the activity of these novel KPI against human neutrophil elastase.

2. Materials and methods

2.1. Analysis of gene structure and protein alignment for single domain KPI of Mylabris variabilis and Lydus trimaculatus

The Trinity-assembled transcripts obtained from the RNAseq data of *Lydus trimaculatus* and *Mylabris variabilis* [35] were used to perform BLAST searches against the corresponding genomes [36]. By convention, each Trinity sequence was considered from the beginning of the transcript up to the STOP codon of the KPI sequence. Gene structures of the Meloidae KPIs were determined using the gene structure display server https://gsds.gao-lab.org [37]. The protein sequences were identified using the Expasy translate tool (https://web.expasy.org/translate/) [38]. Multiple protein sequence alignment was performed with the algorithm implemented in ClustalW (www.ebi.ac.uk/Tools/clustalw/) accessed on 24-04-2025. Phobius website (https://phobius.sbc.su.se/) was used (accessed on 11 January 2021 and 10 June 2022) to predict the presence of signal peptides and the location of their cleavage sites. The aim of the alignment was to highlight conserved residues and domains potentially involved in the functional activity of the peptides. MEROPS cleavage site specificity scoring system available in the MEROPS database (E.C. 3.4.21.37, MEROPS S01.131) were used to analyze the affinity score of each Meloidae KPI considering the amino acid residues located at the P4–P4′ positions.

2.2. Construction of pET17b/ Meloidae KPIs

The cDNAs of the Meloidae KPI that were previously cloned in pCR2.1 vector (TA Cloning Kit, Invitrogen) [38] were subcloned in the expression vector pET17b. Specific primer sets were used to introduce *Nde*I and *Xho*I restriction sites at the 5′ and 3′ ends of meloids KPI cDNA, to introduce the His-tag at the 3′ and to remove the signal peptide at the 5′. See Table 1 for the primer list. The PCR amplicons were digested with the restriction enzymes NdeI and XhoI and ligated with the NdeI/XhoI restricted pET17b vector (Novagen), to obtain the genetic constructs coding for the mature form of the proteins joined to COOH-terminal His-Tag. Thus, the recombinant cDNA constructs were double strand sequenced by Mycrosynth to verify the accuracy of the nucleotide sequences.

2.3. Expression, purification and refolding of Meloidae KPI

Escherichia coli BL21 DE3 was transformed with the expression plasmids pET17b/KPIs. A single transformed colony was inoculated into LB (Luria Bertani) medium containing 100 μg/mL ampicillin and grown overnight at 37 °C with continuous shaking at 200 rpm. The bacterial culture was transferred to fresh LB medium and grown at 37 °C until the OD(600) reached about 0.8. Isopropil-β-D-1-tiogalattopiranoside (IPTG) was then added to a final concentration of 0.5 mM to induce expression of the KPI proteins, and expression was continued at 37 °C for 12 h. The cells were harvested by centrifugation at 4000*g* for 15 min at 4 °C. For purification, a slightly modified protocol according to Sun et al. [39] was performed. Fifteen grams of wet weight cell pellets harvested from 4 L culture medium were suspended in 125 mL binding buffer (20 mM Tris–HCl, 6 M guanidine HCl, 500 mM NaCl, 5 mM imidazole, 10 mM 2-

Table 1
List of the primers used in the study.

Meloidae KPI	Primer for	Primer rev
Lyd_37798 (P1 asp)	5′CTGGAACATATGAGAAGTCCACCAAAACAACAAT3′	5′CTGGAACTCGAGTTAATGATGATGATGATGATGTTGTCGACAAATAGGGATTGC3′
Myl_35212i1 (P1 Leu)	5′CTGGAACATATGGATAATCAAAATAGTGAAAATGAAA3′	5′CTGGAACTCGAGTTAATGATGATGATGATGATGTATATC3′
Myl_17096 (P1 Lys)	5′CTGGAACATATGGATCCGAGGGAATTCTACATAG3′	5′CTGGAACTCGAGTTAATGATGATGATGATGATGCGTACAAATCGGTGTAGC3′
Myl_35212i2 (P1 Phe)	5′CTGGAACATATGGATCAAGATGAATTTACTTTAAATG 3′	5′CTGGAACTCGAGTTAATGATGATGATGATGATGATGTTTCAAACAAATTGG 3′

mercaptoethanol, pH 8.0) and disrupted by pulse sonication on ice. The lysate was centrifuged at 12,000*g* for 25 min at 4 °C, and the supernatant was applied to a Ni-Sepharose column (5 mL) pre-equilibrated with binding buffer. The column was washed one after the other with 5 volumes of binding buffer and then 5 volumes of wash buffer (20 mM Tris–HCl, 8 M urea, 500 mM NaCl, 5 mM imidazole, 10 mM 2-mercaptoethanol, pH 8.0). Then, the proteins were eluted with elution buffer (Tris HCl 20 mM pH 8, Urea 8 M, NaCl 500 mM, imidazole 40 mM, 2-mercaptoethanol 10 mM). Renaturation process was carried out by diluting purified proteins with about 20-fold refolding buffer (50 mM Tris–HCl, 2.5 M urea, 5 mM EDTA, 1.2 mM reduced glutathione, 0.3 mM oxidized glutathione, pH 8.5). After incubation at 10 °C for 72 h, the refolded proteins were extensively dialyzed against the digestion buffer (50 mM Tris–HCl, 100 mM NaCl, pH 8.0). Possible precipitates were removed by centrifugation at 12,000*g* for 20 min at 4 °C. Purified proteins were analyzed by reducing 15 % SDS-polyacrylamide gel electrophoresis (SDS-PAGE) to assess the grade of purification and visualized with Coomassie bright blue R-250. The proteins were concentrated by ultrafiltration with a 3 kDa cut-off membrane (Amicon Centrifugal Filters, Merck Millipore). The concentration of purified proteins were determined by the Bradford procedure [40,41]. The yields of the purification processes were as follows: Lyd_37798 (P1 Asp): 2 mg/L; Myl_17096 (P1 Lys): 5,4 mg/L; Myl_35212i1 (P1 Leu): 5,3 mg/L; Myl_35212i2 (P1 Phe): 8 mg/L.

2.4. Inhibition assays of Meloidae KPI against human neutrophils elastase

Inhibition experiments were performed according to [42] with minor modification. Briefly, reaction was performed in buffer (0.05 M Tris-HCl, pH 8.0) at 37 °C in a flat black bottomed microtiter plate using human neutrophils elastase (NE) (Sigma-Aldrich, CAS: 9004-06-02) at a concentration of 3.5 nM. Different concentrations of Meloidae KPI were pre-incubated for 15 min at room temperature. At the end of the incubation, the reaction was initiated by the addition of the exclusive substrate (Sigma-Aldritch CAS: 72252–90-5, MeOSuc-AAPV-AMC) at a concentration of 140 μM and the absorbance at 460 nm was monitored every 30 s for 30 min at 37 °C with a microplate reader (Tecan Spark 10 M). Controls included in the experiments were: Enzyme plus substrate, Enzyme alone, Substrate alone, and Reaction buffer alone. The inhibitory activities were calculated determining the residual enzymatic activities [43] and the corresponding data elaborated with GraphPad Prism v 8.0.2 according to [44].

2.5. Protein structure prediction and docking analysis

The AlphaFold2 models of KPIs were generated with the ColabFold v1.5.5: AlphaFold2 using MMseqs2 (AlphaFold2.ipynb - ColabFold, accessed on 5 february 2024) [45], without the use of template information. The default mode was used: model_type = alphafold2_ptm, num_recycles = 3, relax_max_interactions = 200, tol = 0.5. To compare AlphaFold-predicted structures with alternative modelling methods, we generated models using Modeller (MODELLER | Bioinformatics Toolkit, accessed 14 July 2023) and SWISS-MODEL (SWISS-MODEL, accessed 01 September 2025). Structural alignments and comparisons were performed using the MatchMaker tool in ChimeraX [46].

Each of the KPI models obtained, and Elafin used as positive control (PDB code: 1FLE, "Chain I"), were docked onto human Neutrophil Elastase (NE, PDB code: 4WVP) using the protein-protein docking software Haddock 2.4 (https://rascar.science.uu.nl/haddock2.4 [47]). Active residue restraints were selected in both NE and KPI models to help guide the protein docking process. Ser195, His57 and Asp102 were indicated as active residues (directly involved in the interaction) for human NE. Default settings were used for docking parameters.

2.6. Expression of ion channels in Xenopus laevis oocytes

Genes encoding for ion channel subunits were expressed in *Xenopus laevis* oocytes: hKv1.1 (KCNA1; NM_000217.3), hKv1.3 (KCNA3; NM_002232.5), hKv7.2/7.3 (KCNQ2/ KCNQ3; NM_004518/ NM_004519), hKv10.1 (EAG1; NM_172362), hKv11.1 (hERG; NM_000238). Linearized plasmids bearing the ion channel genes were transcribed using the mMESSAGE mMACHINE SP6 or T7 transcription kits (Ambion) to prepare the respective cRNA. Oocytes from stage V-VI were harvested from anaesthetized female *X. laevis* frogs as previously described [48]. Adult female were obtained from Nasco (Fort Atkinson, WI, USA) and maintained at the KU Leuven Aquatic Facility under standard conditions, in accordance with the European Union Directive 2010/63/EU. Experimental procedures involving *X. laevis* oocytes were approved by the KU Leuven Animal Ethics Committee (license no. P186/2019). For microinjection, 50 nL of cRNA (1 ng/nL) was delivered into each oocyte using a WPI microinjector (World Precision Instruments (WPI) Sarasota, FL, USA). Following injection, the oocytes were kept at 16 °C in modified Barth's saline solution (88 mM NaCl, 1 mM KCl, 2.5 mM $NaHCO_3$, 1 mM $MgSO_4$, and 5 mM HEPES, pH 7.8), supplemented with 50 mg/L gentamicin sulfate and 90 mg/L theophylline.

2.7. Two-electrode voltage-clamp

Electrophysiological recordings were carried out at room temperature (18 °C–22 °C) using a Geneclamp 500 amplifier (Molecular Devices) connected to a pClamp acquisition system (Axon Instruments). Whole-cell currents were measured in *Xenopus* oocytes between 1 and 4 days following cRNA injection. The external bath solution (ND96) contained: NaCl 2 mM; KCl, 96 mM; $CaCl_2$ 1.8 mM; $MgCl_2$ 2 mM; and HEPES 5 mM (pH 7.4). Electrodes for voltage and current measurements were filled with 3 M KCl. Resistances of both electrodes were kept at 0.7–1.5 MΩ. Elicited currents were sampled at 1 kHz and filtered at 0.5 kHz using a four-pole low-pass Bessel filter. Leak subtraction was performed using a − P/4 protocol.

Kv7.2/7.3 currents were evoked by a 500 ms depolarization to the voltage corresponding to the maximal activation of the channels in control conditions from a holding potential of −90 mV. Recordings of hERG (Kv11.1) channels currents were obtained using a protocol that applied a 2 s depolarizing pulse from −90 mV to +40 mV, followed by a repolarizing step to −120 mV for 2 s. Kv10.1 currents were evoked by 2 s depolarizing pulses to 0 mV from a holding potential of −90 mV. Kv1.1 and Kv1.3 currents were evoked by 500 ms depolarizations to 0 mV followed by a 500 ms pulse to −50 mV from a holding potential of −90 mV. All samples were applied directly into the bath, in a final concentration of 8 μM for Myl_17096 (P1 Lys), 1.5 μM for Myl_35212i1 (P1 Leu) and 1 μM for Lyd_37798 (P1 Asp). All data were obtained in at least three independent experiments ($n \geq 3$).

2.8. Neutrophil isolation

Peripheral blood lymphocytes were isolated from buffy coat of healthy male blood donors (45–50 years old).

To isolate neutrophils, human blood was diluted with Phosphate Buffered saline (PBS) and then layered on 10 mL of Ficoll-Hypaque solution (Amersham Biosciences, GE Healthcare Europe GmbH, Glattbrugg, Switzerland). After a centrifugation (230 xg at 20 °C for 20 min) the bottom layer (red blood cells and neutrophils) was carefully harvested and mixed with 3 % dextran solution (Sigma-Aldrich, St. Louis, MO, USA) at a 1:1 ratio, gently inverted 20 times to ensure adequate mixing, and incubated at 25 °C for 1 h.

Once the different phases were clearly layered, the top layer was carefully transferred and centrifuged at 1100× rpm at 4 °C for 8 min. The obtained pellet was resuspended in 1 mL PBS, then 10 mL of 0.2 % NaCl solution was added and left for 20 s, then the same volume of 1.6 % NaCl solution was quickly added, and the tube was inverted.

After washing twice with cold PBS, the final pellets were resuspended in RPMI media containing 3 % fetal bovine serum (FBS) to obtain a final concentration of 5×10^6 neutrophils/mL [49,50].

2.9. Neutrophils extracellular traps (NETs) generation

NETosis was induced as previously described [49,50]. Briefly, neutrophils were stimulated with 500 nM of phorbol myristate acetate (PMA). 10 µg/mL of Meloidae KPI (Myl_17096 (P1 Lys); Lys_37,798 (P1 Asp); Myl_35212i1 (P1 Leu) and Myl_35212i2 (P1 Phe)) were added and incubated on a 150 × 25 mm flat tissue culture dish for 4 h at 37 °C and 5 % CO_2. After the stimulation, the culture medium was gently aspirated and discarded, taking great care not to destroy or compromise the layer of NETs and neutrophils at the bottom of the culture dishes. All adherent material was then lifted off using cold PBS (15 mL, without Ca^{++} and Mg^{++}) and carefully collected in a 15 mL conical tube. A centrifugation (10 min at 450 xg at 4 °C) selectively pelleted neutrophils and any remaining cells at the bottom, leaving a cell-free NET-rich supernatant in the upper layer. To collect all the DNA, supernatants were centrifuged (10 min at 18,000 x g at 4 °C). DNA pellets were resuspended in ice cold PBS to a concentration corresponding to about 2×10^7 neutrophils per 100 µL of PBS. DNA concentration was then assessed spectrophotometrically at 260 nm.

3. Results

3.1. Characterization of genes of the new Kunitz peptide inhibitors from transcriptomic and genomic analysis of L. trimaculatus and M. variabilis

Next generation sequencing (NGS)-based transcriptome analyses of adult specimens of *L. trimaculatus* and *M. variabilis* performed by Fratini et al. [35] revealed several transcripts associated with the regulation of coagulation in the whole body, in the accessory gland, and in the hemolymph. From this dataset, 15 sequences containing a single Kunitz-Type domain were identified and 9 of them were cloned [38]. Recently, a novel genome assembly of the two species [36] allowed the integration of transcriptomic and genomic data. mRNA sequences were aligned to the genome, allowing us to identify the gene structures and organization of the Meloidae derived KPI gene loci (Fig. 1). With this approach, as shown in Fig. 1, we could point out nine single kunitz domain genes in the two species, six in *M. variabilis* and three in *L. trimaculatus*. All of them, except for *Lyd_46461*, have a structure made of two exons separated by a small intron. Two transcripts, *Lyd_46461* and *Lyd_34901*, partially overlap in the genome and likely represent two splicing variants of the same gene. This hypothesis is also supported by the analysis of the nucleotide and amino acid sequences, showing that the transcript Lyd_46461 lacks the signal peptide, a common feature of KPIs [38]. *Myl_35212i1* and *Myl_35212i2*, *Myl_37778* and *Myl_21616g1/2* are located in tandem on the scaffolds 175 and 353, respectively.

To investigate the inhibitory specificity of the newly identified Kunitz-type peptides, we selected four peptides on the base of their P1 residue for recombinant expression in *Escherichia coli*. The selected peptides Myl_17096 (P1 Lys), Myl_35212i2 (P1 Phe), Myl_35212i1 (P1 Leu), and Lyd_37798 (P1 Asp) were chosen to represent a broad spectrum of physicochemical properties, including basic, aromatic, hydrophobic, and acidic side chains. This strategic selection enabled us to assess how distinct P1 residues modulate binding affinity and inhibitory activity toward neutrophil elastase. The multiple sequence alignment highlighting the position and nature of the P1 residues and the

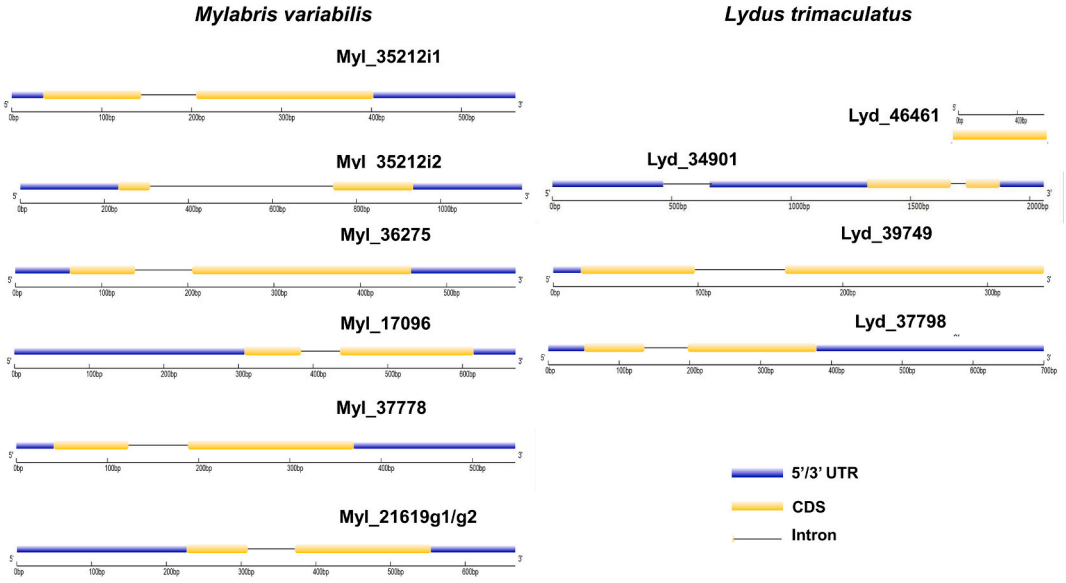

Fig. 1. Gene structures of Meloidae Kunitz-type protease inhibitors (KPIs). Gene structures of single domain Meloidae KPIs were determined using the server https://gsds.gao-lab.org. On the left are reported the six genes identified in the genome of *Mylabris variabilis*, on the right the three genes identified in the genome of *Lydus trimaculatus*. Exons are represented as yellow boxes, 5′ and 3′ untraslated region (UTR) as blue boxes and introns as black lines. Scale bars represent nucleotide length. Lyd_46461 is represented as an alternative exon in the Lyd_34901 gene. (For interpretation of the references to colour in this figure legend, the reader is referred to the web version of this article.)

sequences comparison with known Kunitz peptides is shown in Fig. 2. Considering the amino acid residues located at the P4–P4′ positions of the selected Kunitz peptides Lyd_37798 (Asp), Myl_35212i1 (Leu), Myl_17096 (Lys), and Myl_35212i2 (Phe) we evaluated their potential interactions with NE by applying the cleavage site specificity scoring system available in the MEROPS database [2]. This analysis enabled us to predict the relative inhibitory tendencies of each peptide toward NE. The outcomes of this scoring procedure are presented in Supplementary Table S1, offering a comparative overview of the distinct inhibitory capacities associated with the different peptide variants.

3.2. Expression of Meloidae Kunitz peptides

Utilizing the program Phobius (see Section 2) [51] 16–17 amino acids long N-terminal putative signal sequences were identified in the coding sequence of the selected Kunitz proteins [38] (Fig. 2). These signal peptides were removed from the corresponding cDNAs and a His-Tag coding sequence was added to their C-terminal end (see Section 2). The cDNAs coding for these mutated proteins were subcloned in the expression vector plasmid pET17b and the transformed positive clones were utilized for the heterologous expression in the *E. coli* BL21 DE3 strain. The recombinant proteins were then purified by His-Bind chromatography and their purity was assessed by SDS/PAGE electrophoretic analysis (Fig. 3).

3.3. Inhibition specificity of Meloidae Kunitz peptides on the activities of neutrophil elastase

In order to evaluate the potential of *Meloidae* KPI to inhibit NE, *in vitro* enzymatic assays were performed. Different peptides concentrations were incubated with human NE (at a concentration of 3.5 nM) and its substrate (at a concentration of 140 μM) as described in the Section 2. The four *Meloidae* KPI showed different ability to inhibit NE enzymatic activity (Fig. 4 and Table 2) and apparent inhibition constants (Ki app) were as follows: Lyd_37798 (P1 Asp) 32.36 ± 5 nM, Myl_35212i1 (P1 Leu) 76.45 ± 7 nM, Myl_17096 (P1 Lys) 154.5 ± 13,8 nM and Myl_35212i2 (P1 Phe) 754.3 ± 93 nM.

3.4. Molecular docking of the Kunitz peptides with NE

Structural models of the *Meloidae* KPI obtained using AlphaFold2 and validated on Modeller and SWISS-Model predicted structures (see Section 2 and Supplementary Table S2) confirmed that the inhibitors display the canonical Cys-framework with a I–VI, II–IV and III–V connectivity [38]. To investigate the structural basis of the inhibition properties of the *Meloidae* KPI, the protein-protein docking software Haddock 2.4 was used to obtain the molecular models of their complexes

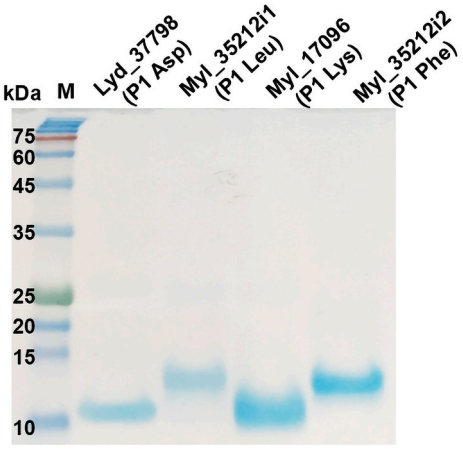

Fig. 3. Coomassie Blue stained SDS PAGE of purified recombinant Meloidae KPI. Coomassie Blue stained SDS PAGE showing purified recombinant Meloidae KPI. kDa: kilo Dalton; M: molecular weight ladder. (For interpretation of the references to colour in this figure legend, the reader is referred to the web version of this article.)

with NE (see Section 2). Fig. 5 displays the highest scoring model complex for each KPI. Comparative analysis of the complexes obtained by docking with the experimental structure of porcine pancreatic elastase bound to the specific inhibitor Elafin (PDB code 1FLE; [52]) evidences that the most effective inhibitors Lyd_37798 (P1 Asp) and Myl_35212i1 (P1 Leu) are predicted to bind with their reactive loop almost perfectly superimposable to that of Elafin and the P1 residue in exactly the same position of the Ala P1 residue of the specific inhibitor (Fig. 5B and C). Conversely, the Myl_17096 (P1 Lys) and Myl_35212i2 (P1 Phe) inhibitors display a different conformation of the reactive loop and much looser interactions with the enzyme active site (Fig. 5D and E). The same docking analysis was performed using Elafin as a positive control (PDB code 1FLE, chain I). The docking-generated Elafin–elastase model aligns almost perfectly with the crystal structure of the Elafin–elastase complex (Fig. 5A). Analysis of the experimental structure of the elastase-Elafin complex (PDB code 1FLE) evidence that the inhibitor reactive loop makes extensive van der Waals contacts with the enzyme's active site crevice. In addition, the P1 residue Ala of the inhibitor is inserted in the hydrophobic S1 pocket facing Val216 (Fig. 5, panel A). A similar arrangement of the reactive loop is observed in the Lyd_37798 (P1 Asp) and Myl_35212i1 (P1 Leu) complexes (Fig. 5, panels B and C, respectively), with the P1 residue Asp of the Lyd_37798 inhibitor establishing electrostatic interactions with the catalytic Ser195 residue of the enzyme and the P1 residue Leu of the Myl_35212i1 inserted in the

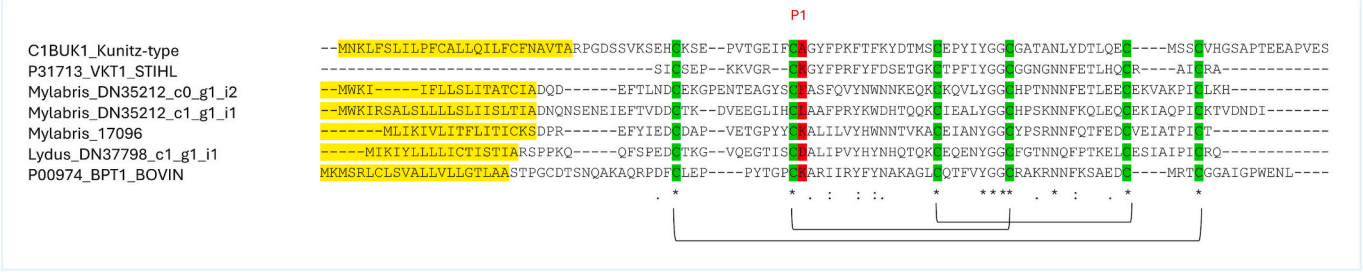

Fig. 2. ClustalW multiple sequence alignment of Meloidae Kunitz protein. The alignment of the aminoacidic sequences of Lyd_37798 (P1 Asp), Myl_35212i1 (P1 Leu), Myl_17096 (P1 Lys), and Myl_35212i2 (P1 Phe) with the kunitz sequences Pancreatic trypsin inhibitor (uniport code: P00974 · BPT1_BOVIN), Kunitz-type proteinase inhibitor SHPI-1 (uniport code: C1BUK1 · C1BUK1_LEPSM) and PI-stichotoxin-She2a (uniport code: P31713 · VKT1_STIHL) are reported. Yellow, leader sequence. Green, cysteines involved in the Kunitz disulphide bridges (highlighted by black crosslinks). Red, P1 site. Consensus key: "*" indicates positions which have fully conserved residues; ":" indicates conserved positions containing residues with strongly similar properties; "." indicates conserved positions with residues possessing weakly similar properties; blank spaces mean no consensus. (For interpretation of the references to colour in this figure legend, the reader is referred to the web version of this article.)

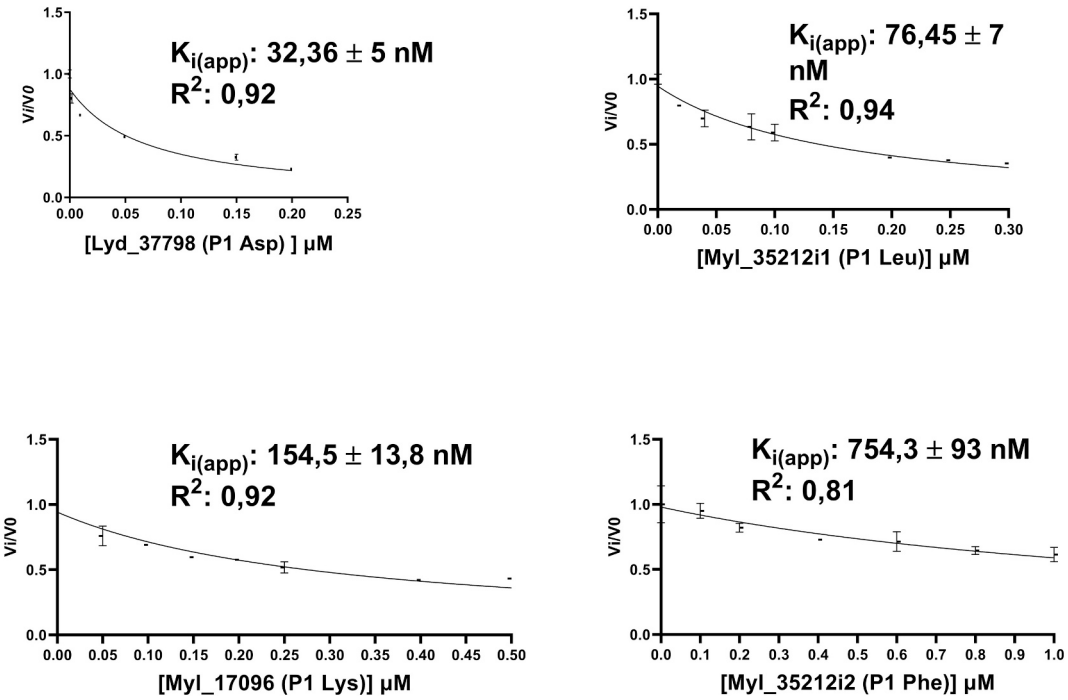

Fig. 4. Inhibitory curve of Meloidae KPI toward human neutrophil elastase. Different concentrations of the Meloidae KPI were incubated with human neutrophil elastase (3.5 nM), followed by the addition of chromogenic substrate (140 µM). The ratio of velocities of substrate hydrolysis in the presence (Vi) and in the absence (Vo) of different concentrations of Meloidae KPI is plotted, showing the relative inhibition. Different range of inhibitor concentration were tested for the Meloidae KPI. Ki (app) and R^2 for each inhibitor are reported in the graphs.

Table 2
Inhibition constant (Ki) of the Meloidae KPI and human neutrophil elastase.

KPI	Ki (nM)	R^2
Lyd_37798 (P1 asp)	32.36 ± 4	0.92
Myl_35212i1 (P1 Leu)	76.45 ± 7	0.94
Myl_17096 (P1 Lys)	154.5 ± 13.8	0.92
Myl_35212i2 (P1 Phe)	754.3 ± 93	0.81

hydrophobic S1 site in contact with Val 216. In contrast, the Myl_17096 (P1 Lys) and, to a higher extent, the Myl_35212i2 (P1 Phe) inhibitors are predicted to bind at the periphery of the active site crevice with a very limited contact surface, a result that is fully in line with their much lower affinity for the enzyme.

3.5. Effect of Kunitz-type protease inhibitors on NETs generation

To further analyze the activity of *Meloidae* KPI in a cellular context, we incubated them with activated neutrophils from healthy donors (HD) and measured the neutrophils extracellular trap (NET) formation. To this end, neutrophils were stimulated with PMA (500 nM for 4 h) to induce NETs generation (compared to untreated cells 301.3 ± 76.3 fold increase, $p < 0.0001$). Co-administration of *Meloidae* KPI with PMA induced different results depending on the type of peptide tested (Fig. 6).

The most pronounced inhibition of NETosis was observed with the peptides Lyd_37798 (P1 Asp) and Myl_17096 (P1 Lys), showing reductions of 88.8 % and 86.8 %, respectively, compared to PMA stimulation ($p < 0.0001$). A statistically significant, though more moderate, inhibitory effect was also observed with Myl_35212i1 (P1 Leu) and Myl_35212i2 (P1 Phe), which reduced NET formation by 57.9 % ($p < 0.001$) and 13.5 % ($p < 0.01$) (Fig. 6). These findings are consistent with the *in vitro* assays, confirming that Lyd_37798 (Asp), Myl_17096 (Lys), and Myl_35212i1 (Leu) are the most potent Meloidae KPIs against human NE.

3.6. Activity toward Kv channels: electrophysiological recordings

Dendrotoxins are small proteins that were isolated 20 years ago from mamba (Dendroaspis) snake venoms [53] and shown to be homologous to Kunitz-type serine protease inhibitors, such as bovine pancreatic trypsin inhibitor. The dendrotoxins have little or no antiprotease activity, but they were demonstrated to block particular subtypes of voltage-dependent potassium channels (Kv1.x) in neurons (for a review, see [54]). Moreover, recent findings showed that Kv1.3 participate in the regulation of neutrophil activity during acute inflammatory processes [55] and thus it would be important to address if Meloidae KPIs could have more than one target in the context of neutrophil activation. To evaluate the inhibitory potential of the newly identified Meloidae KPIs on different voltage-gated potassium channels, we expressed different channels in *Xenopus laevis* oocytes and measured the KPI activity using the two-electrode voltage clamp (TEVC) technique (Fig. 7). The three peptides that showed the maximum inhibitory efficacy *versus* NE (Lyd_37798 (P1 Asp), Myl_17096 (P1 Lys) and Myl_35212i1 (P1 Leu)) were tested on Kv1.1 and Kv1.3 isoforms, whereby several Kv1.x isoforms are known to be blocked with high affinity (IC_{50} in the nanomolar range). As shown in Fig. 7A and B lack of activity has been recorded against Kv1.1 and Kv1.3 isoforms. In order to check if the three peptides showed activity against other voltage-gated potassium channels, we tested also Kv7.2/7.3 heteromeric, Kv10.1 and Kv11.1 channels for the following reasons: i)the pharmacology of Kv7.2/7.3 channels remains largely unexplored in the domains where they are natively expressed; ii) among all ion channels, Kv10.1 has been established as a promising target in cancer treatment due to the high expression in tumoral tissues compared to low levels in healthy tissues; iii) Kv11.1 mediates repolarization of cardiac action potentials in humans and loss of function mutations cause inheritable long QT syndrome, characterized by a prolonged QT interval and an increased risk of ventricular arrhythmia. To the best of our knowledge, KPI activity has not been reported for the above mentioned targets. Lyd_37798 (P1 Asp), Myl_17096 (P1 Lys) and Myl_35212i1 (P1 Leu) were tested on voltage-

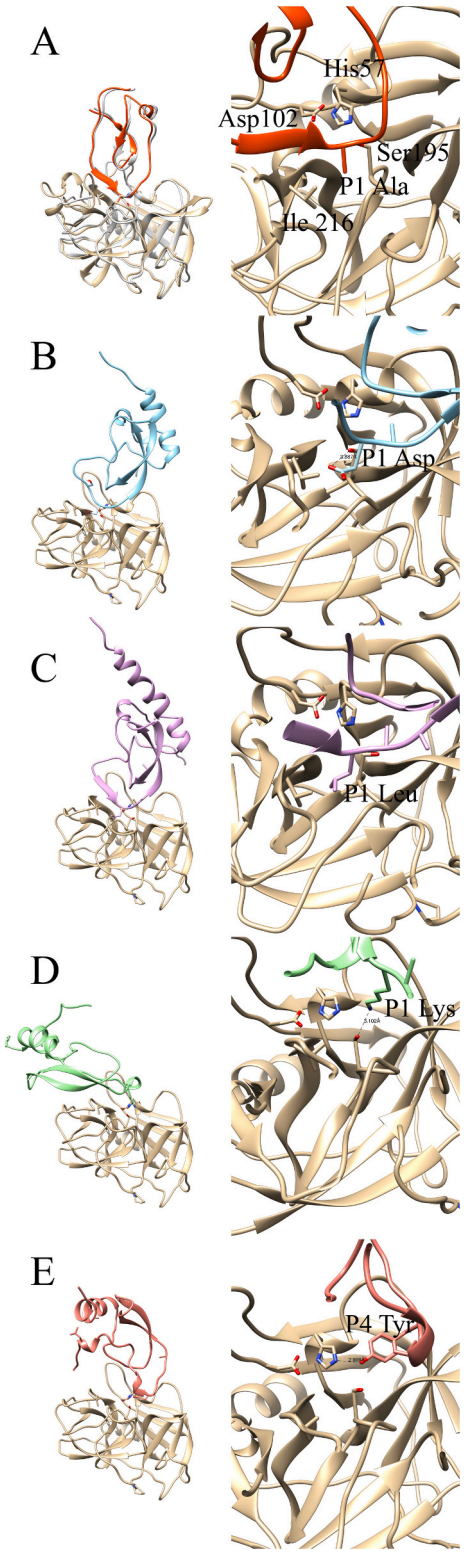

(caption on next column)

Fig. 5. Structural details of the experimental and predicted enzyme-inhibitors complexes. Left panels display a general view of the complexes while right panels display an enlarged view of the proteases active site regions. Labels indicate the protease catalytic triad residues (Ser195, His57, Asp102), the Val216 residue located in the S1 specificity site and the P1 residues of each inhibitor (P4 in the case of Myl_35212i2 (P1 Phe; see below)). (A) Experimental structure of the porcine pancreatic elastase (light brown ribbon) bound to the specific inhibitor Elafin (orange ribbon) (PDB code IFLE; [25]). The structural model of the complex between Elafin and the human Neutrophil Elastase (light grey ribbon), used as a positive control, is also shown superimposed onto the experimental structure; (B) Lyd_37798 (P1 Asp). The dashed line indicates the electrostatic interaction between the carboxyl group of the P1 Asp residue and the catalytic triad Ser195 residue; (C) Myl_35212i1 (P1 Leu). From the figure it can be seen that the P1 Leu residue is predicted to form a hydrophobic interaction with Leu216; (D) Myl_17096 (P1 Lys). The figure clearly shows the peripheral binding mode predicted for this inhibitor, the only interaction observed being a hydrogen bond (dashed line) between the P1 Lys residue of the inhibitor and the catalytic triad Ser residue; (E) Myl_35212i2 (P1 Phe). Also in this case, docking simulations predict a very loose binding mode between the inhibitor and the enzyme, the only significant interaction observed being a hydrogen bond between the P4 Tyr residue of the inhibitor and the catalytic triad His residue (dashed line). (For interpretation of the references to colour in this figure legend, the reader is referred to the web version of this article.)

gated potassium channels Kv7.2/7.3, Kv10.1, and Kv11.1 and no activity was observed (Fig. 7C and D). These results suggest a specificity of the Meloidae Kunitz peptides toward NE.

4. Discussion

Transcriptomic and genomic analyses conducted in two species of Meloidae insects allowed the identification of 15 single domain Kunitz transcripts, corresponding to nine distinct genes, six in *Mylabris variabilis* and three in *Lydus trimaculatus*. These genes show a similar organization and, in some cases, are arranged in tandem in the genome, leading to the hypothesis of extensive evolutionary diversification from a common ancestral gene (Fig. 1).

The high number of KPIs found in Meloidae reflects their importance for the physiology of these insects but also highlights how Meloidae can represent a reservoir of peptides with potential pharmacological interest. Through the comparison of mRNAs and genomic sequences, we reconstructed the gene architecture and mapped the organization of the KPI gene loci (Fig. 1). Most genes share a conserved structure of two exons separated by a short intron, except for *Lyd_46461*, which appears to lack the signal peptide typically found in KPIs. Based on their genomic overlap and sequence similarity, *Lyd_46461* and *Lyd_34901* may represent alternative splicing variants of a single locus. Additionally, we observed tandem arrangements of several KPI genes (*Myl_35212i1/i2*, *Myl_37778*, and *Myl_21616g1/2*) on specific scaffolds, suggesting possible gene duplication events. This interesting evolutionary aspect could reflect the necessity of insects to widen the panel of protease inhibitors directed at multiple targets.

To functionally characterize these inhibitors, we selected four peptides for recombinant expression in *E. coli* based on the identity of their P1 residue. The chosen candidates Myl_17096 (P1 Lys), Myl_35212i2 (P1 Phe), Myl_35212i1 (P1 Leu), and Lyd_37798 (P1 Asp) show a range of physicochemical profiles (basic, aromatic, hydrophobic, and acidic), allowing us to explore how P1 variation influences inhibitory activity against NE. The multiple sequence alignment presented in Fig. 2 illustrates the sequence diversity and P1 positioning of the analyzed inhibitors in comparison with other extensively characterized members of the Kunitz family.

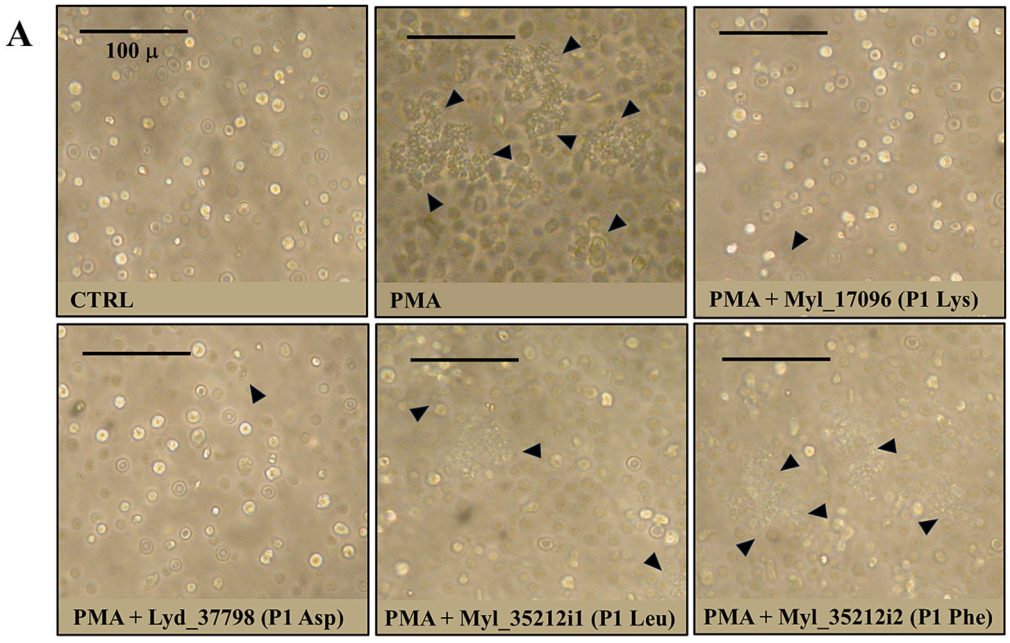

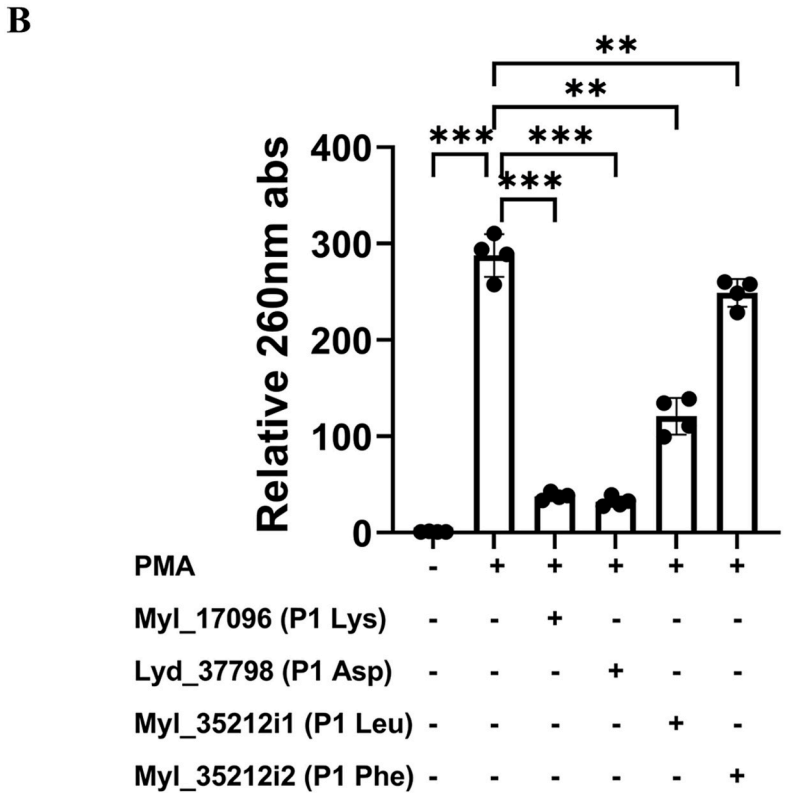

Fig. 6. Effect of Meloidae KPI on NETs generation. Human neutrophils from male healthy donors were stimulated with 500 nM of PMA in single or combined treatments with peptides (Myl_17096 (Lys); Lyd_ 37,798 (Asp); Myl_35212i1 (Leu) and Myl_35212i2 (Phe)) for 4 h. (A) After the treatment period, cells were observed under the microscope and the generation of NETs was detected (black arrows). The images are representative of the experiments performed. The black bar indicates the size of 100 µm. (B) Spectrophotometrical absorbance at 260 nm of the pellet indicating the extracellular DNA (see the Section 2). The graph represents the ratio between the absorbance of each sample and the mean of the non-stimulated samples. The experiments were performed four times. One-way ANOVA with Tukey post-hoc test has been applied, $^{**}p < 0.01$, $^{***}p < 0.001$.

In KPIs targeting elastase, the P1 residue plays a critical role in determining specificity and binding affinity. Structural studies have demonstrated that hydrophobic amino acids, particularly leucine (Leu), are commonly found at the P1 position in KPIs effective against elastase. This preference is due to the structural characteristics of elastase's S1 pocket, which is optimally suited to adapt side chains that are small or medium in size and hydrophobic in nature. Notably, the substitution of the P1 residue with leucine in the KPI inhibitor has been shown to

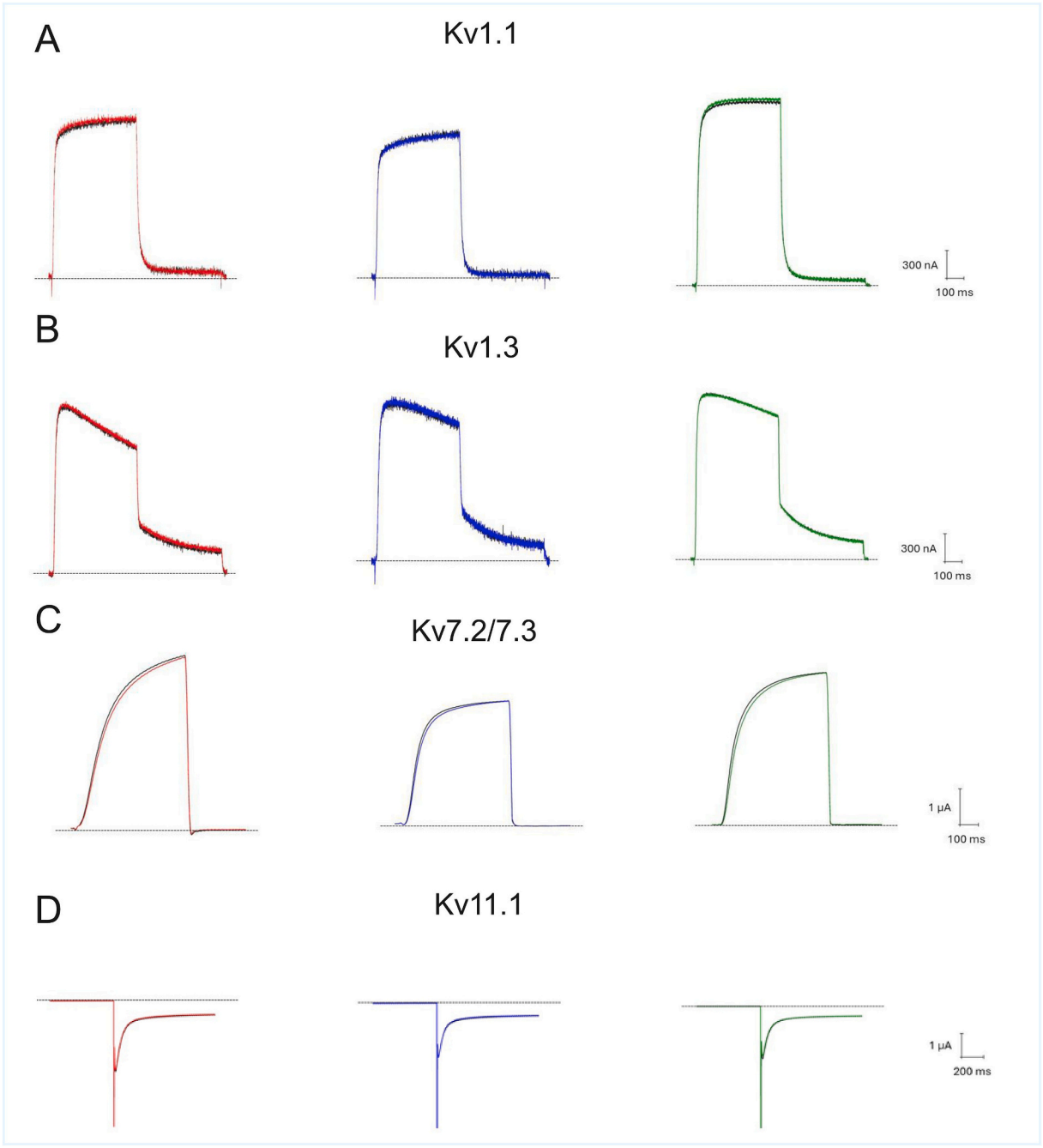

Fig. 7. Activity of Lyd_37798 (P1 Asp), of Myl_17096 (P1Lys) and of Myl_35212i1 (P1 Leu) toward Kv channels. Meloidae KPI, Myl_17096 (P1 Lys) reported in red, Myl_35212i1 (P1 Leu) reported in blue and Lyd_37798 (P1 Asp) reported in green were applied directly into the bath *containing X. laevis* oocytes transfected with cDNA codifying for the reported ion channel subunits. Recording of control are reported as black lines. (A) voltage-gated potassium channel 1.1 (Kv1.1), (B) voltage-gated potassium channel 1.3 (Kv1.3), (C) voltage-gated potassium channel 7.2/7.3 (Kv7.2/7.3) and (D) human Ether-a-go-go-related Gene potassium channel (hERG/Kv11.1). All data were obtained in at least three independent experiments ($n \geq 3$). (For interpretation of the references to colour in this figure legend, the reader is referred to the web version of this article.)

markedly increase the affinity for elastase, converting it into a tight-binding inhibitor with nanomolar affinity [4,21,56,57].

In contrast, KPIs with basic residues like lysine (Lys) or arginine (Arg) at the P1 position tend to exhibit higher specificity toward trypsin-like proteases rather than elastase. This distinction highlights the importance of the P1 residue's characteristics in designing KPIs with desired specificity [4,58] When designing or evaluating KPIs targeting elastase, prioritizing hydrophobic P1 residues, particularly Leu, has proven to be a strategic choice to enhance inhibitory efficacy [56]. Consistent with this rationale, the peptide Myl_35212i1 (P1 Leu), bearing a leucine at the P1 position, demonstrated strong elastase inhibition (Fig. 4). Intriguingly, the most potent inhibitor in our study was Lyd_37798 (P1 Asp), which features an aspartic acid at P1, a residue type not commonly associated with elastase inhibitors. This unexpected result opens new avenues for considering acidic residues in KPI design, challenging the conventional preference for hydrophobicity at this position. However, protease specificity in KPIs is not dictated solely by the P1 residue; rather, it arises from a combination of interactions involving multiple amino acids within the conserved Kunitz domain [57]. When evaluating the amino acid residues at the P4–P4′ positions of the selected

Kunitz peptides (Lyd_37798, Myl_35212i1, Myl_17096, and Myl_35212i2), the scoring matrix from the MEROPS database [2] predicted inhibitory preferences (Supplementary Table S1) that were fully consistent with the experimentally determined Ki values (Fig. 4). Notably, the analysis emphasizes the critical role of residues at the P4–P4' sites in shaping peptide–enzyme interactions. This concordance not only reinforces the robustness of our experimental findings but also underscores the utility of integrating computational scoring with biochemical assays to guide rational peptide design. In a broader context, such insights may prove valuable for the development of tailored peptide-based inhibitors with therapeutic potential against protease-driven pathologies. To further elucidate the molecular basis underlying these observations, particularly the superior inhibitory capacity of Lyd_37798 (P1 Asp) and Myl_35212i1 (P1 Leu), we performed molecular modelling analyses. Structural inspection of the experimental elastase–Elafin complex (PDB code 1FLE) highlights that the inhibitor's reactive loop establishes extensive van der Waals contacts within the enzyme's active site crevice. Furthermore, the P1 Ala residue of Elafin is tightly accommodated within the hydrophobic S1 pocket, positioned opposite to Val216 (Fig. 5, panel A). A comparable arrangement was observed in the Lyd_37798 (P1 Asp) and Myl_35212i1 (P1 Leu) complexes (Fig. 5, panels B and C, respectively): the P1 Asp residue of Lyd_37798 engages in electrostatic interactions with the catalytic Ser195, whereas the P1 Leu residue of Myl_35212i1 fits snugly into the hydrophobic S1 site, contacting Val216. By contrast, the binding modes of Myl_17096 and, more markedly, Myl_35212i2 are shifted toward the periphery of the active site cleft, resulting in a reduced interaction surface area. This structural evidence is in excellent agreement with their lower experimentally measured affinities for elastase. Elafin is involved in inflammatory disease and is receiving great attention as a potential candidate for the anti-inflammatory treatment of respiratory diseases [59]. The identification of two new Kunitz peptides with a similar mechanism of binding of Elafin is of strong pharmacological interest. It would be important to perform structural and mutagenesis analyses to increase our knowledge of Elafin, Lyd_37798 (P1 Asp), and Myl_35212i1 (P1 Leu) mode of action to improve their pharmacological properties. To extend the functional relevance of our biodiversity-inspired Kunitz inhibitors, we evaluated their ability to suppress NETosis, a process implicated in various inflammatory pathologies associated with excessive neutrophil activation (Fig. 6). Neutrophils from healthy donors were stimulated with PMA to induce NET formation, and co-incubated with selected Meloidae KPIs. The peptides Lyd_37798 (P1 Asp) and Myl_17096 (P1 Lys) exhibited the strongest inhibitory effects, suppressing NET release by nearly 90 %. Myl_35212i1 (P1 Leu) and Myl_35212i2 (P1 Phe) also reduced NET formation, though their effects were more modest. Overall, Lyd_37798 (P1 Asp) stood out as the most efficient compound, acting as both the most potent elastase inhibitor and the most effective blocker of NETosis, suggesting promising therapeutic potential. In addition to NE, other proteases contribute to NET formation, among them proteinase 3 (PR3 or myeloblastin), cathepsin G (CatG) and neutrophil serine protease 4 (NSP4) [60–62]. We cannot exclude that Meloidae KPIs exert their inhibitor effects also on those proteases. This is particularly true for Myl_17096 (P1 Lys), which shows a strong NET inhibition in cellular tests but a Ki *versus* NE of about 150 nM. It is interesting to note that, NSP4 is a trypsin-like enzyme and thus can be inhibited by KPI with a positively charged P1 residue, such as lysine or arginine [63]. Thus, it would be interesting in the future to assess if Meloidae KPIs are active also against other neutrophil proteases.

We also tested the ability of Meloidae KPI to inhibit potassium voltage channels (Fig. 7), since there are some reported proteins with both functions of inhibiting serine proteases and blocking potassium channels [4,64,65] and because a role for some Kv channels (especially Kv 1.3) has been emerging in the regulation of neutrophils activation [55]. This aspect could be of great pharmacological interest in the inflammatory disorders characterized by excessive neutrophil infiltration. The complete lack of inhibition toward the voltage gated channels tested restricted the potential pharmacological use of Meloidae KPIs but on the other hand highlight the specificity of these new peptides, strengthening the interest in their use as potential elastase inhibitor drugs.

The need to find new NE inhibitors arises from their increasing use in the prevention of adverse effects of diseases characterized by a violent inflammatory response such as acute respiratory distress syndrome (ARDS), induced by excessive NE activation [66,67]. NE directly activates inflammation by increasing cytokine expression and release and indirectly by triggering extracellular trap and exosome release, thereby amplifying protease activity and inflammation [68,69]. Clinical therapies that utilize protease inhibitors in controlling sepsis and related inflammatory disorders are limited, with the use of urinary trypsin inhibitor (UTI) [70], also called ulinastatin or bikunin, being the only approved option. UTI is a naturally occurring multivalent Kunitz-type inhibitor with notable anti-inflammatory effects [71]. Beyond inflammation, there are strong evidence that, in various cancers, the secretion of various proteases correlates with the aggressiveness of the tumour. Indeed, some KPI such as Bikunin [72], Tissue Factor Pathway Inhibitor-2 (TFPI-2) [73] and Serine Peptidase Inhibitor, Kunitz Type 2 (SPINT2) [74] have been demonstrated to inhibit cancer progression suggesting that modulation of protease activity may have therapeutic applications in both inflammation and oncology. However, neutrophils and NE can also counteract tumour progression for example by inducing the death of tumour cells while sparing proximal healthy cells [18,75]. Thus, the role of NE and of KPI in the tumour context needs to be evaluated in depth and considered case by case.

The use of natural peptides derived from meloids insects can represent a repertoire for therapeutic purposes, also considering that protease inhibitors of natural origin often have greater therapeutic potential and fewer side effects than synthetic ones [76–78]. Moreover, the Kunitz peptides act as reversible inhibitors that are usually preferred over irreversible ones [76]. Compared to other Kunitz inhibitors that are components of the venom, Meloidea derived KPI show the advantage to be evolved to regulate the organism's own processes probably presenting more specificity and less toxicity.

In addition, several Kunitz inhibitors are already available as drugs for the prevention and treatment of specific diseases, such as ecallantide (approved for hereditary angioedema [79]) and aprotinin (used during medical or surgical procedures to avoid the risk of bleeding [80]).

We recognize some aspects in our study that deserve further investigation. First, although we did not directly assess the refolding efficiency of our purification method, it is possible that a fraction of the purified KPI may not have been fully folded, which could result in a conservative estimate of the activity *versus* NE. Second, we tested the Meloidae-derived KPIs against a selected panel of ion channels, and additional proteases were not included. It would be important in the future to provide a more comprehensive characterization of the specificity and explore the potential broader activity of each new Meloidae-derived KPIs. Moreover, future investigation will be essential to delineate the molecular mechanisms underlying the activity of Kunitz-type elastase inhibitors. Novel target-discovery platforms, including proteolysis-targeting chimera (PROTAC) probe technologies and state-of-the-art proteomic approaches, provide promising opportunities to identify interacting partners and clarify the downstream pathways modulated by these inhibitors [81]. The application of such methodologies may significantly advance our understanding of their pharmacological profile and open avenues for the development of next-generation therapeutic strategies.

In conclusion, the discovery of Meloidae Kunitz-type inhibitors opens new avenues for the development of innovative drugs against NE. Their potential application in the inflammation control and in the modulation of cancer-related protease activity makes them as compelling candidates for future drug development in both inflammatory and oncological settings.

CRediT authorship contribution statement

Marianna Nicoletta Rossi: Writing – review & editing, Writing – original draft, Validation, Project administration, Methodology, Formal analysis, Conceptualization. **Lavinia Attili:** Writing – review & editing, Investigation, Formal analysis. **Cristian Fiorucci:** Writing – review & editing, Investigation, Formal analysis. **William Fabiani:** Writing – review & editing, Investigation. **Sarah Andreucci:** Writing – review & editing, Investigation, Formal analysis. **Paolo Franchini:** Writing – review & editing, Software, Data curation. **Alessandra Riccieri:** Writing – review & editing, Resources, Investigation. **Lucrezia Spagoni:** Writing – review & editing, Resources, Investigation. **Marco Alberto Bologna:** Writing – review & editing, Resources, Funding acquisition. **Guglielmo Duranti:** Writing – review & editing, Resources, Methodology, Investigation, Funding acquisition. **Roberta Ceci:** Writing – review & editing, Resources, Methodology, Funding acquisition. **Emiliano Fratini:** Writing – review & editing, Software, Data curation. **Kathleen Carleer:** Writing – review & editing, Investigation. **Jan Tytgat:** Writing – review & editing, Resources, Project administration, Methodology, Investigation. **Fabio Polticelli:** Writing – review & editing, Software, Funding acquisition, Data curation. **Manuela Cervelli:** Writing – review & editing, Writing – original draft, Validation, Project administration, Methodology, Funding acquisition, Formal analysis, Conceptualization.

Funding

This research was financed by the project "NuOvi farmaCi anticoaguLanti dalla biOdiversiTà dei meloidi—NO CLOT" financed by Regione Lazio, Bandi per Gruppi di Ricerca 2020, grant number A0375-2020-36555, and by MUR-Italy Grants of Departments of Excellence—L. 232/2016—art.1 cc. 314-337 awarded to the Department of Science of Roma Tre University (2023–2027). Financial support by Project ECS 0000024 Rome Technopole, – NRP Mission 4 Component 2 Investment 1.5, Funded by the European Union – NextGenerationEU is gratefully acknowledged.

Declaration of competing interest

The authors declare that they have no known competing financial interests or personal relationships that could have influenced the work reported in this paper.

Acknowledgments

The authors thanks prof Emiliano Mancini for valuable suggestions and discussion.

Declaration of competing interest

The authors declare that they have no known competing financial interests or personal relationships that could have appeared to influence the work reported in this paper.

Appendix A. Supplementary data

Supplementary data to this article can be found online at https://doi.org/10.1016/j.bioorg.2025.109128.

Data availability

Data shared with a private link.
Meloidae KPI versus elastase (Original data) (Figshare)

References

[1] M. Kunitz, Crystallization of a trypsin inhibitor from soybean, Science 101 (1945) 668–669, https://doi.org/10.1126/science.101.2635.668.
[2] N.D. Rawlings, A. Bateman, How to use the *MEROPS* database and website to help understand peptidase specificity, Protein Sci. 30 (2021) 83–92, https://doi.org/10.1002/pro.3948.
[3] N.D. Rawlings, M. Waller, A.J. Barrett, A. Bateman, *MEROPS* : the database of proteolytic enzymes, their substrates and inhibitors, Nucleic Acids Res. 42 (2014) D503–D509, https://doi.org/10.1093/nar/gkt953.
[4] M. Mishra, Evolutionary aspects of the structural convergence and functional diversification of Kunitz-domain inhibitors, J. Mol. Evol. 88 (2020) 537–548, https://doi.org/10.1007/s00239-020-09959-9.
[5] S. Ranasinghe, D.P. McManus, Structure and function of invertebrate Kunitz serine protease inhibitors, Dev. Comp. Immunol. 39 (2013) 219–227, https://doi.org/10.1016/j.dci.2012.10.005.
[6] W. Zeng, Y. Song, R. Wang, R. He, T. Wang, Neutrophil elastase: from mechanisms to therapeutic potential, J. Pharm. Anal. 13 (2023) 355–366, https://doi.org/10.1016/j.jpha.2022.12.003.
[7] V. Brinkmann, U. Reichard, C. Goosmann, B. Fauler, Y. Uhlemann, D.S. Weiss, Y. Weinrauch, A. Zychlinsky, Neutrophil extracellular traps kill Bacteria, Science 303 (2004) 1532–1535, https://doi.org/10.1126/science.1092385.
[8] S.K. Jorch, P. Kubes, An emerging role for neutrophil extracellular traps in noninfectious disease, Nat. Med. 23 (2017) 279–287, https://doi.org/10.1038/nm.4294.
[9] A.A. Baz, H. Hao, S. Lan, Z. Li, S. Liu, S. Chen, Y. Chu, Neutrophil extracellular traps in bacterial infections and evasion strategies, Front. Immunol. 15 (2024) 1357967, https://doi.org/10.3389/fimmu.2024.1357967.
[10] G. Pignataro, S. Gemma, M. Petrucci, F. Barone, A. Piccioni, F. Franceschi, M. Candelli, Unraveling NETs in Sepsis: from cellular mechanisms to clinical relevance, I.J.M.S. 26 (2025) 7464, https://doi.org/10.3390/ijms26157464.
[11] A. Belaaouaj, R. McCarthy, M. Baumann, Z. Gao, T.J. Ley, S.N. Abraham, S. D. Shapiro, Mice lacking neutrophil elastase reveal impaired host defense against gram negative bacterial sepsis, Nat. Med. 4 (1998) 615–618, https://doi.org/10.1038/nm0598-615.
[12] G. Orriols, C. Aljama, F. Rodriguez-Frias, P.-G. Medina, R. Ferrer-Costa, G. Granados, A. Nuñez, A. López-González, G. Ruiz-Satelinas, M. Miravitlles, M. Barrecheguren, C. Esquinas, Quantification of serum elastase inhibitory activity in patients with pulmonary emphysema with and without alpha-1 antitrypsin deficiency, PLoS ONE 20 (2025) e0324237, https://doi.org/10.1371/journal.pone.0324237.
[13] E.A. Middleton, X.-Y. He, F. Denorme, R.A. Campbell, D. Ng, S.P. Salvatore, M. Mostyka, A. Baxter-Stoltzfus, A.C. Borczuk, M. Loda, M.J. Cody, B.K. Manne, I. Portier, E.S. Harris, A.C. Petrey, E.J. Beswick, A.F. Caulin, A. Iovino, L. M. Abegglen, A.S. Weyrich, M.T. Rondina, M. Egeblad, J.D. Schiffman, C.C. Yost, Neutrophil extracellular traps contribute to immunothrombosis in COVID-19 acute respiratory distress syndrome, Blood 136 (2020) 1169–1179, https://doi.org/10.1182/blood.2020007008.
[14] M. Ackermann, S.E. Verleden, M. Kuehnel, A. Haverich, T. Welte, F. Laenger, A. Vanstapel, C. Werlein, H. Stark, A. Tzankov, W.W. Li, V.W. Li, S.J. Mentzer, D. Jonigk, Pulmonary vascular Endothelialitis, thrombosis, and angiogenesis in Covid-19, N. Engl. J. Med. 383 (2020) 120–128, https://doi.org/10.1056/NEJMoa2015432.
[15] B.J. Barnes, J.M. Adrover, A. Baxter-Stoltzfus, A. Borczuk, J. Cools-Lartigue, J. M. Crawford, J. Daßler-Plenker, P. Guerci, C. Huynh, J.S. Knight, M. Loda, M. R. Looney, F. McAllister, R. Rayes, S. Renaud, S. Rousseau, S. Salvatore, R. E. Schwartz, J.D. Spicer, C.C. Yost, A. Weber, Y. Zuo, M. Egeblad, Targeting potential drivers of COVID-19: neutrophil extracellular traps, J. Exp. Med. 217 (2020) e20200652, https://doi.org/10.1084/jem.20200652.
[16] Y. Zuo, S. Yalavarthi, H. Shi, K. Gockman, M. Zuo, J.A. Madison, C.N. Blair, A. Weber, B.J. Barnes, M. Egeblad, R.J. Woods, Y. Kanthi, J.S. Knight, Neutrophil extracellular traps in COVID-19, JCI Insight (2020), https://doi.org/10.1172/jci.insight.138999.
[17] J.A. Aoki, F. Denorme, M.J. Cody, D.P. Perry, J.L. Rustad, S.M. Brown, S. A. Goldstein, E.A. Middleton, C.C. Yost, E.S. Harris, for the NHLBI prevention and early treatment of acute lung injury (PETAL) network investigators, plasma surrogate markers of neutrophil extracellular traps correlate with disease severity in patients with moderate to severe acute respiratory distress syndrome, J. Inflamm. 22 (2025) 22, https://doi.org/10.1186/s12950-025-00448-8.
[18] G. Favaretto, M.N. Rossi, L. Cuollo, M. Laffranchi, M. Cervelli, A. Soriani, S. Sozzani, A. Santoni, F. Antonangeli, Neutrophil-activating secretome characterizes palbociclib-induced senescence of breast cancer cells, Cancer Immunol. Immunother. 73 (2024) 113, https://doi.org/10.1007/s00262-024-03695-5.
[19] C.J. Wagner, C. Schultz, M.A. Mall, Neutrophil elastase and matrix metalloproteinase 12 in cystic fibrosis lung disease, Mol. Cell. Pediatr. 3 (2016) 25, https://doi.org/10.1186/s40348-016-0053-7.
[20] A.S. Dittrich, I. Kühbandner, S. Gehrig, V. Rickert-Zacharias, M. Twigg, S. Wege, C. C. Taggart, F. Herth, C. Schultz, M.A. Mall, Elastase activity on sputum neutrophils correlates with severity of lung disease in cystic fibrosis, Eur. Respir. J. 51 (2018) 1701910, https://doi.org/10.1183/13993003.01910-2017.
[21] V.D. Giacalone, C. Margaroli, M.A. Mall, R. Tirouvanziam, Neutrophil adaptations upon recruitment to the lung: new concepts and implications for homeostasis and disease, I.J.M.S. 21 (2020) 851, https://doi.org/10.3390/ijms21030851.
[22] J.D. Chalmers, M.A. Mall, S.H. Chotirmall, A.E. O'Donnell, P.A. Flume, N. Hasegawa, F.C. Ringshausen, H. Watz, J.-F. Xu, M. Shteinberg, P.J. McShane,

Targeting neutrophil serine proteases in bronchiectasis, Eur. Respir. J. 65 (2025) 2401050, https://doi.org/10.1183/13993003.01050-2024.
[23] M.R. Kanost, Serine proteinase inhibitors in arthropod immunity, Dev. Comp. Immunol. 23 (1999) 291–301, https://doi.org/10.1016/S0145-305X(99)00012-9.
[24] G. Li, L. Yang, K. Xiao, Q. Song, D. Stanley, S. Wei, J. Zhu, Characterization and expression profiling of serine protease inhibitors in the yellow mealworm *Tenebrio molitor*, Arch. Insect Biochem. Physiol. 111 (2022) e21948, https://doi.org/10.1002/arch.21948.
[25] J. Heng, H. Liu, J. Xu, X. Huang, X. Sun, R. Yang, Q. Xia, P. Zhao, KPI5 is involved in the regulation of the expression of antibacterial peptide genes and hemolymph Melanization in the silkworm, Bombyx mori, Front. Immunol. 13 (2022) 907427, https://doi.org/10.3389/fimmu.2022.907427.
[26] M.A. Jmel, H. Voet, R.N. Araújo, L. Tirloni, A. Sá-Nunes, M. Kotsyfakis, Tick salivary Kunitz-type inhibitors: targeting host hemostasis and immunity to mediate successful blood feeding, I.J.M.S. 24 (2023) 1556, https://doi.org/10.3390/ijms24021556.
[27] G.C. Ferreira, L.D.M. Bomediano Camillo, S.D. Sasaki, Structural and functional properties of rBmTI-a: A Kunitz-BPTI serine protease inhibitor with therapeutical potential, Biochimie 204 (2023) 1–7, https://doi.org/10.1016/j.biochi.2022.08.004.
[28] P.C. Valenzuela-Leon, A. Campos Chagas, I. Martin-Martin, A.E. Williams, M. Berger, G. Shrivastava, A.S. Paige, M. Kotsyfakis, L. Tirloni, E. Calvo, Guianensin, a Simulium guianense salivary protein, has broad anti-hemostatic and anti-inflammatory properties, Front. Immunol. 14 (2023) 1163367, https://doi.org/10.3389/fimmu.2023.1163367.
[29] L. Fahmy, T. Generalovic, Y.M. Ali, D. Seilly, K. Sivanesan, L. Kalmar, M. Pipan, G. Christie, A.J. Grant, A novel family of defensin-like peptides from Hermetia illucens with antibacterial properties, BMC Microbiol. 24 (2024) 167, https://doi.org/10.1186/s12866-024-03325-1.
[30] Y. He, Z. Li, L. Wei, Z. Wang, Y. Shen, X. Wang, X. Yang, L. Mu, H. Yang, J. Wu, Sibanin, a novel black fly-derived Kunitz protease inhibitor, prevents thrombus formation in mice by anticoagulation-antiplatelet duality, Int. J. Biol. Macromol. 296 (2025) 139766, https://doi.org/10.1016/j.ijbiomac.2025.139766.
[31] H. Lin, X. Lin, J. Zhu, X.-Q. Yu, X. Xia, F. Yao, G. Yang, M. You, Characterization and expression profiling of serine protease inhibitors in the diamondback moth, Plutella xylostella (Lepidoptera: Plutellidae), BMC Genomics 18 (2017) 162, https://doi.org/10.1186/s12864-017-3583-z.
[32] M.A. Bologna, B. D'Inzillo, M. Cervelli, M. Oliverio, P. Mariottini, Molecular phylogenetic studies of the Mylabrini blister beetles (Coleoptera, Meloidae), Mol. Phylogenet. Evol. 37 (2005) 306–311, https://doi.org/10.1016/j.ympev.2005.03.034.
[33] M.A. Bologna, F. Turco, J.D. Pinto, 11.19. Meloidae Gyllenhal, 1810, in: W. Kükenthal, R.A.B. Leschen, R.G. Beutel, J.F. Lawrence (Eds.), Coleoptera, Beetles, Volume 2, Morphology and Systematics (Elateroidea, Bostrichiformia, Cucujiformia Partim), DE GRUYTER, 2010, pp. 681–693, https://doi.org/10.1515/9783110911213.681.
[34] C.R. Bonturi, A.B. Silva Teixeira, V.M. Rocha, P.F. Valente, J.R. Oliveira, C.M. B. Filho, I. Fátima Correia Batista, M.L.V. Oliva, Plant Kunitz inhibitors and their interaction with proteases: current and potential pharmacological targets, I.J.M.S. 23 (2022) 4742, https://doi.org/10.3390/ijms23094742.
[35] E. Fratini, M. Salvemini, F. Lombardo, M. Muzzi, M. Molfini, S. Gisondi, E. Roma, V. D'Ezio, T. Persichini, T. Gasperi, P. Mariottini, A. Di Giulio, M.A. Bologna, M. Cervelli, E. Mancini, Unraveling the role of male reproductive tract and haemolymph in cantharidin-exuding Lydus trimaculatus and Mylabris variabilis (Coleoptera: Meloidae): a comparative transcriptomics approach, BMC Genomics 22 (2021) 808, https://doi.org/10.1186/s12864-021-08118-8.
[36] A. Riccieri, L. Spagoni, M. Li, P. Franchini, M.N. Rossi, E. Fratini, M. Cervelli, M. A. Bologna, E. Mancini, Comparative genomics provides insights into molecular adaptation to hypermetamorphosis and cantharidin metabolism in blister beetles (Coleoptera: Meloidae), Integr. Zool. 19 (2024) 975–988, https://doi.org/10.1111/1749-4877.12819.
[37] A.-Y. Guo, Q.-H. Zhu, X. Chen, J.-C. Luo, [GSDS: a gene structure display server], [software], Yi Chuan 29 (2007) 1023–1026.
[38] E. Fratini, M.N. Rossi, L. Spagoni, A. Riccieri, E. Mancini, F. Polticelli, M. A. Bologna, P. Mariottini, M. Cervelli, Molecular characterization of Kunitz-type protease inhibitors from blister beetles (Coleoptera, Meloidae), Biomolecules 12 (2022) 988, https://doi.org/10.3390/biom12070988.
[39] L. Sun, S. Wang, X. Gong, M. Zhao, X. Fu, L. Wang, Isolation, purification and characteristics of R-phycoerythrin from a marine macroalga Heterosiphonia japonica, Protein Expr. Purif. 64 (2009) 146–154, https://doi.org/10.1016/j.pep.2008.09.013.
[40] M.M. Bradford, A rapid and sensitive method for the quantitation of microgram quantities of protein utilizing the principle of protein-dye binding, Anal. Biochem. 72 (1976) 248–254, https://doi.org/10.1016/0003-2697(76)90527-3.
[41] S. Pietropaoli, A. Leonetti, C. Cervetto, A. Venturini, R. Mastrantonio, G. Baroli, T. Persichini, M. Colasanti, G. Maura, M. Marcoli, P. Mariottini, M. Cervelli, Glutamate excitotoxicity linked to Spermine oxidase overexpression, Mol. Neurobiol. 55 (2018) 7259–7270, https://doi.org/10.1007/s12035-017-0864-0.
[42] I. Cruz-Silva, A.J. Gozzo, V.A. Nunes, A.S. Tanaka, M. Da Silva Araujo, Bioengineering of an elastase inhibitor from Caesalpinia echinata (Brazil wood) seeds, Phytochemistry 182 (2021) 112595, https://doi.org/10.1016/j.phytochem.2020.112595.
[43] J.F. Morrison, The slow-binding and slow, tight-binding inhibition of enzyme-catalysed reactions, T.I.B.S. 7 (1982) 102–105, https://doi.org/10.1016/0968-0004(82)90157-8.
[44] R. García-Fernández, S. Peigneur, T. Pons, C. Alvarez, L. González, M. Chávez, J. Tytgat, The Kunitz-type protein ShPI-1 inhibits serine proteases and voltage-gated potassium channels, Toxins 8 (2016) 110, https://doi.org/10.3390/toxins8040110.
[45] M. Mirdita, K. Schütze, Y. Moriwaki, L. Heo, S. Ovchinnikov, M. Steinegger, ColabFold: making protein folding accessible to all, Nat. Methods 19 (2022) 679–682, https://doi.org/10.1038/s41592-022-01488-1.
[46] E.C. Meng, T.D. Goddard, E.F. Pettersen, G.S. Couch, Z.J. Pearson, J.H. Morris, T. E. Ferrin, UCSF ChimeraX : tools for structure building and analysis, Protein Sci. 32 (2023) e4792, https://doi.org/10.1002/pro.4792.
[47] G.C.P. Van Zundert, J.P.G.L.M. Rodrigues, M. Trellet, C. Schmitz, P.L. Kastritis, E. Karaca, A.S.J. Melquiond, M. Van Dijk, S.J. De Vries, A.M.J.J. Bonvin, The HADDOCK2.2 web server: user-friendly integrative modeling of biomolecular complexes, J. Mol. Biol. 428 (2016) 720–725, https://doi.org/10.1016/j.jmb.2015.09.014.
[48] S. Peigneur, C. Da Costa Oliveira, F.C. De Sousa Fonseca, K.L. McMahon, A. Mueller, O. Cheneval, A. Cristina Nogueira Freitas, H. Starobova, I. Dimitri Gama Duarte, D.J. Craik, I. Vetter, M.E. De Lima, C.I. Schroeder, J. Tytgat, Small cyclic sodium channel inhibitors, Biochem. Pharmacol. 183 (2021) 114291, https://doi.org/10.1016/j.bcp.2020.114291.
[49] S. Najmeh, J. Cools-Lartigue, B. Giannias, J. Spicer, L.E. Ferri, Simplified human neutrophil extracellular traps (NETs) isolation and handling, JoVE (2015) 52687, https://doi.org/10.3791/52687-v.
[50] Y.-C. Kim, S.E. Lee, S.K. Kim, H.-D. Jang, I. Hwang, S. Jin, E.-B. Hong, K.-S. Jang, H.-S. Kim, Toll-like receptor mediated inflammation requires FASN-dependent MYD88 palmitoylation, Nat. Chem. Biol. 15 (2019) 907–916, https://doi.org/10.1038/s41589-019-0344-0.
[51] L. Käll, A. Krogh, E.L.L. Sonnhammer, A combined transmembrane topology and signal peptide prediction method, J. Mol. Biol. 338 (2004) 1027–1036, https://doi.org/10.1016/j.jmb.2004.03.016.
[52] M. Tsunemi, Y. Matsuura, S. Sakakibara, Y. Katsube, Crystal structure of an elastase-specific inhibitor Elafin complexed with porcine pancreatic elastase determined at 1.9 Å resolution, Biochemistry 35 (1996) 11570–11576, https://doi.org/10.1021/bi9609001.
[53] A.L. Harvey, E. Karlsson, Dendrotoxin from the venom of the green mamba, Dendroaspis angusticeps: a neurotoxin that enhances acetylcholine release at neuromuscular junctions, Naunyn-Schmiedeberg's, Arch. Pharmacol. 312 (1980) 1–6, https://doi.org/10.1007/BF00502565.
[54] A.L. Harvey, Twenty years of dendrotoxins, Toxicon 39 (2001) 15–26, https://doi.org/10.1016/S0041-0101(00)00162-8.
[55] R. Immler, W. Nadolni, A. Bertsch, V. Morikis, I. Rohwedder, S. Masgrau-Alsina, T. Schroll, A. Yevtushenko, O. Soehnlein, M. Moser, T. Gudermann, E.R. Barnea, M. Rehberg, S.I. Simon, S. Zierler, M. Pruenster, M. Sperandio, The voltage-gated potassium channel KV1.3 regulates neutrophil recruitment during inflammation, Cardiovasc. Res. 118 (2022) 1289–1302, https://doi.org/10.1093/cvr/cvab133.
[56] R. García-Fernández, M. Perbandt, D. Rehders, P. Ziegelmüller, N. Piganeau, U. Hahn, C. Betzel, M.D.L.Á. Chávez, L. Redecke, Three-dimensional structure of a Kunitz-type inhibitor in complex with an elastase-like enzyme, J. Biol. Chem. 290 (2015) 14154–14165, https://doi.org/10.1074/jbc.M115.647586.
[57] E.I. Millers, M. Trabi, P.P. Masci, M.F. Lavin, J. De Jersey, L.W. Guddat, Crystal structure of textilinin-1, a Kunitz-type serine protease inhibitor from the venom of the Australian common brown snake (*Pseudonaja textilis*), FEBS J. 276 (2009) 3163–3175, https://doi.org/10.1111/j.1742-4658.2009.07034.x.
[58] H. Jering, H. Tschesche, Replacement of lysine by arginine, phenylalanine and tryptophan in the reactive site of the bovine trypsin-Kallikrein inhibitor (Kunitz) and change of the inhibitory properties, Eur. J. Biochem. 61 (1976) 453–463, https://doi.org/10.1111/j.1432-1033.1976.tb10039.x.
[59] M. He, Y. Yang, Y. Li, X. Zhou, L. Xu, Z. Zhang, H. Zhang, Q. Li, Therapeutic potential of elafin in airway inflammatory disease, Eur. J. Inflamm. 22 (2024) 1721727X241237437, https://doi.org/10.1177/1721727X241237437.
[60] A. Korba-Mikołajczyk, K.D. Służalska, P. Kasperkiewicz, Exploring the involvement of serine proteases in neutrophil extracellular traps: a review of mechanisms and implications, Cell Death Dis. 16 (2025) 535, https://doi.org/10.1038/s41419-025-07857-w.
[61] N.C. Perera, O. Schilling, H. Kittel, W. Back, E. Kremmer, D.E. Jenne, NSP4, an elastase-related protease in human neutrophils with arginine specificity, Proc. Natl. Acad. Sci. USA 109 (2012) 6229–6234, https://doi.org/10.1073/pnas.1200470109.
[62] M. Skoreński, K. Torzyk, M. Sieńczyk, Neutrophil serine proteases, Rare Dis. Orphan. Drugs J. 2 (2023) 6, https://doi.org/10.20517/rdodj.2022.21.
[63] P. Ascenzi, A. Bocedi, M. Bolognesi, A. Spallarossa, M. Coletta, R. Cristofaro, E. Menegatti, The bovine basic pancreatic trypsin inhibitor (Kunitz inhibitor): a milestone protein, CPPS 4 (2003) 231–251, https://doi.org/10.2174/1389203033487180.
[64] J. Ciolek, H. Reinfrank, L. Quinton, S. Viengchareun, E.A. Stura, L. Vera, S. Sigismeau, B. Mouillac, H. Orcel, S. Peigneur, J. Tytgat, L. Droctové, F. Beau, J. Nevoux, M. Lombès, G. Mourier, E. De Pauw, D. Servent, C. Mendre, R. Witzgall, N. Gilles, Green mamba peptide targets type-2 vasopressin receptor against polycystic kidney disease, Proc. Natl. Acad. Sci. USA 114 (2017) 7154–7159, https://doi.org/10.1073/pnas.1620454114.
[65] S. Peigneur, B. Billen, R. Derua, E. Waelkens, S. Debaveye, L. Béress, J. Tytgat, A bifunctional sea anemone peptide with Kunitz type protease and potassium channel inhibiting properties, Biochem. Pharmacol. 82 (2011) 81–90, https://doi.org/10.1016/j.bcp.2011.03.023.
[66] M.C. Cesta, M. Zippoli, C. Marsiglia, E.M. Gavioli, G. Cremonesi, A. Khan, F. Mantelli, M. Allegretti, R. Balk, Neutrophil activation and neutrophil

extracellular traps (NETs) in COVID-19 ARDS and immunothrombosis, Eur. J. Immunol. 53 (2023) 2250010, https://doi.org/10.1002/eji.202250010.
[67] C.-C. Chiang, M. Korinek, W.-J. Cheng, T.-L. Hwang, Targeting neutrophils to treat acute respiratory distress syndrome in coronavirus disease, Front. Pharmacol. 11 (2020) 572009, https://doi.org/10.3389/fphar.2020.572009.
[68] B. Korkmaz, M.S. Horwitz, D.E. Jenne, F. Gauthier, Neutrophil elastase, proteinase 3, and Cathepsin G as therapeutic targets in human diseases, Pharmacol. Rev. 62 (2010) 726–759, https://doi.org/10.1124/pr.110.002733.
[69] S.D. Lucas, E. Costa, R.C. Guedes, R. Moreira, Targeting COPD: advances on low-molecular-weight inhibitors of human neutrophil elastase, Med. Res. Rev. 33 (2013), https://doi.org/10.1002/med.20247.
[70] K. Inoue, H. Takano, Urinary trypsin inhibitor as a therapeutic option for endotoxin-related inflammatory disorders, Expert Opin. Investig. Drugs 19 (2010) 513–520, https://doi.org/10.1517/13543781003649533.
[71] S.-H. Lee, H. Kim, H.-J. Han, M. Li, S.-H. Kwak, S. Park, Urinary trypsin inhibitor attenuates lipopolysaccharide-induced neutrophil activation, Korean J. Anesthesiol. 63 (2012) 540, https://doi.org/10.4097/kjae.2012.63.6.540.
[72] H. Kobayashi, M. Suzuki, Y. Tanaka, N. Kanayama, T. Terao, A Kunitz-type protease inhibitor, Bikunin, inhibits ovarian Cancer cell invasion by blocking the calcium-dependent transforming growth factor-β1 signaling Cascade, J. Biol. Chem. 278 (2003) 7790–7799, https://doi.org/10.1074/jbc.M210407200.
[73] E. Sierko, M. Wojtukiewicz, W. Kisiel, The role of tissue factor pathway Inhibitor-2 in Cancer biology, Semin. Thromb. Hemost. 33 (2007) 653–659, https://doi.org/10.1055/s-2007-991532.
[74] P.N. Kongkham, P.A. Northcott, Y.S. Ra, Y. Nakahara, T.G. Mainprize, S.E. Croul, C.A. Smith, M.D. Taylor, J.T. Rutka, An epigenetic genome-wide screen identifies *SPINT2* as a novel tumor suppressor gene in pediatric Medulloblastoma, Cancer Res. 68 (2008) 9945–9953, https://doi.org/10.1158/0008-5472.CAN-08-2169.
[75] C. Cui, K. Chakraborty, X.A. Tang, G. Zhou, K.Q. Schoenfelt, K.M. Becker, A. Hoffman, Y.-F. Chang, A. Blank, C.A. Reardon, H.A. Kenny, T. Vaisar, E. Lengyel, G. Greene, L. Becker, Neutrophil elastase selectively kills cancer cells and attenuates tumorigenesis, Cell 184 (2021) 3163–3177.e21, https://doi.org/10.1016/j.cell.2021.04.016.
[76] D.S. Johnson, E. Weerapana, B.F. Cravatt, Strategies for discovering and Derisking covalent, irreversible enzyme inhibitors, future, Med. Chem. 2 (2010) 949–964, https://doi.org/10.4155/fmc.10.21.
[77] C. Junren, X. Xiaofang, Z. Huiqiong, L. Gangmin, Y. Yanpeng, C. Xiaoyu, G. Yuqing, L. Yanan, Z. Yue, P. Fu, P. Cheng, Pharmacological activities and mechanisms of Hirudin and its derivatives - a review, Front. Pharmacol. 12 (2021) 660757, https://doi.org/10.3389/fphar.2021.660757.
[78] A.A. Stoop, C.S. Craik, Engineering of a macromolecular scaffold to develop specific protease inhibitors, Nat. Biotechnol. 21 (2003) 1063–1068, https://doi.org/10.1038/nbt860.
[79] J.A. Bernstein, J.J. Moellman, S.P. Collins, K.W. Hart, C.J. Lindsell, Effectiveness of ecallantide in treating angiotensin-converting enzyme inhibitor–induced angioedema in the emergency department, Ann. Allergy Asthma Immunol. 114 (2015) 245–249, https://doi.org/10.1016/j.anai.2014.12.007.
[80] A.M. Mahdy, N.R. Webster, Perioperative systemic haemostatic agents, Br. J. Anaesth. 93 (2004) 842–858, https://doi.org/10.1093/bja/aeh227.
[81] S. Yan, G. Zhang, W. Luo, M. Xu, R. Peng, Z. Du, Y. Liu, Z. Bai, X. Xiao, S. Qin, PROTAC technology: from drug development to probe technology for target deconvolution, Eur. J. Med. Chem. 276 (2024) 116725, https://doi.org/10.1016/j.ejmech.2024.116725.